AGU PUBLICATIONS

Geophysical Research Letters

RESEARCH LETTER
10.1002/2015GL065161

Key Point:
- Strong carbon sink observed with GOSAT in Australia during 2010–2011

Correspondence to:
R. G. Detmers,
r.g.detmers@sron.nl

Citation:
Detmers, R. G., O. Hasekamp, I. Aben, S. Houweling, T. T. van Leeuwen, A. Butz, J. Landgraf, P. Köhler, L. Guanter, and B. Poulter (2015), Anomalous carbon uptake in Australia as seen by GOSAT, *Geophys. Res. Lett.*, *42*, 8177–8184, doi:10.1002/2015GL065161.

Received 1 JUL 2015
Accepted 1 SEP 2015
Accepted article online 7 SEP 2015
Published online 5 OCT 2015

Anomalous carbon uptake in Australia as seen by GOSAT

R. G. Detmers[1], O. Hasekamp[1], I. Aben[1], S. Houweling[1,2], T. T. van Leeuwen[1,2], A. Butz[3], J. Landgraf[1], P. Köhler[4], L. Guanter[4], and B. Poulter[5]

[1]SRON Netherlands Institute for Space Research, Utrecht, Netherlands, [2]Institute for Marine and Atmospheric Research, Utrecht University, Utrecht, Netherlands, [3]Karlsruhe Institute of Technology, Karlsruhe, Germany, [4]Helmholtz Centre Potsdam, GFZ German Research Centre for Geosciences, Potsdam, Germany, [5]Institute on Ecosystems and Department of Ecology, Montana State University, Bozeman, Montana, USA

Abstract One of the unanswered questions of climate change is how the biospheric uptake of carbon responds to events such as droughts and floods. Especially, semiarid regions have received interest recently, as they can respond very rapidly to changing environmental conditions. Here we report on a large enhanced carbon sink over Australia from the end of 2010 to early 2012 detected using the Greenhouse Gases Observing SATellite (GOSAT). This enhanced sink coincides with the strong La Niña episode, accompanied by record-breaking amounts of precipitation. This precipitation led to an enhanced growth of vegetation, resulting in large increases in biospheric carbon uptake in line with increased levels of vegetation fluorescence. An inversion based on the satellite retrievals confirms this strong anomaly in the sink of roughly 0.77 ± 0.10 Pg C yr^{-1} or 1.5 ± 0.2 Pg C in total for the April 2010 to December 2011 period, which corresponds to 25% of the multiyear annual average gross primary production of the Australian biosphere.

1. Introduction

Variability in the observed growth rate of atmospheric carbon dioxide (CO_2) has recently been linked mostly to variations in the terrestrial ecosystem uptake [*Cox et al.*, 2013]. These interannual variations can be up to 1–2 ppm (Dr. Pieter Tans, NOAA/ESRL (www.esrl.noaa.gov/gmd/ccgg/trends/)) and even larger on regional scales. What drives these variations is not entirely clear yet, as drought/flooding, temperature, fire emissions, and land use changes can all play a significant role in changing the carbon land sink of a region [*Keppel-Aleks et al.*, 2014]. The focus of most studies has previously been on tropical rainforests as the main driver for changes in the land carbon uptake [*Cox et al.*, 2013; *Wang et al.*, 2013]. Recently, however, several studies have shown the importance of semiarid regions in the CO_2 interannual variability [*Rotenberg and Yakir*, 2010; *Poulter et al.*, 2014]. Due to the soil moisture-limited nature of these regions, the response to drought and flooding conditions can be fast and large. An anomaly in the carbon uptake of 1.3 ± 0.6 Pg C yr^{-1} was estimated for 2011 in *Poulter et al.* [2014], driven almost purely by uptake in semiarid regions of the Southern Hemisphere.

Dynamic global vegetation models that describe these processes, such as Organizing Carbon and Hydrology in Dynamic Ecosystems (http://orchidee.ipsl.jussieu.fr) or the Lund-Potsdam-Jena (LPJ) model [*Sitch et al.*, 2003], still contain many uncertainties and can differ significantly between each other [*Keenan et al.*, 2012]. Satellite remote sensing, with its global coverage, can be a valuable tool to study the carbon cycle either by observing the CO_2 concentration directly or by deriving other indirectly related parameters (e.g., plant fluorescence). Greenhouse Gases Observing Satellite (GOSAT) and the recently launched Orbiting Carbon Observatory-2 are the only two satellites currently capable of providing total column measurements of CO_2 [*Butz et al.*, 2011; *Yoshida et al.*, 2011; *Crisp et al.*, 2012; *Frankenberg et al.*, 2015]. By combining these total column observations with additional measurements such as soil moisture and normalized difference vegetation index (NDVI) and inserting these observations in an inversion system, such as the TM5-4DVAR system [*Meirink et al.*, 2008; *Basu et al.*, 2011], we can better understand the underlying processes and adjust or possibly improve the biochemical models.

An important semiarid region from a carbon perspective is Australia, where most of the vegetation in the interior consists of grasses and shrubs (see Figure 1). In the past few decades a general decrease in precipitation in parts of Southern Australia has been observed [*Delworth and Zeng*, 2014]. Also, 2009 and early 2010 were very dry years due to a strong El Niño. At the end of 2010, however, this shifted dramatically as the combined effect of a strong La Niña with enhancing influences from the Indian Ocean Dipole and Southern Annular

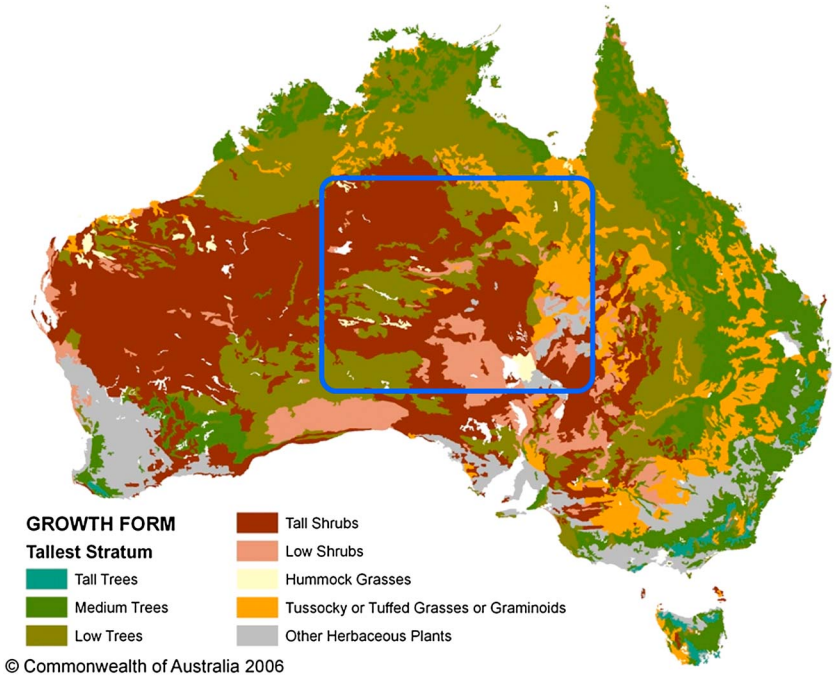

Figure 1. Vegetation map of Australia, with the central region marked in blue. Source: Australian Bureau of Agricultural and Resource Economics and Sciences.

Mode causing record-breaking precipitation over large parts of Australia. This lasted well into 2012 and has been associated with a global 7 mm drop in the ocean levels [*Fasullo et al.*, 2013]. This led to a large increase in observed net primary production (NPP) in 2011 [*Bastos et al.*, 2013]. As NPP is tightly coupled to the carbon land sink, this should have a strong effect on the carbon uptake in Australia, especially in the central region, where the effect of enhanced soil moisture is expected to be strongest.

We analyzed GOSAT total column average dry-air mole fraction of atmospheric carbon dioxide for CO_2 (XCO_2) measurements over Australia from the period 2009–2013, in order to investigate the effects of the large precipitation anomalies during that period on the carbon cycle. These data were then correlated against several parameters that connect to the underlying processes (soil moisture and fluorescence) and compared to model data. The corresponding anomaly in the CO_2 exchange flux has been quantified by means of the satellite-based TM5-4DVAR inversion system. Our paper is organized in the following way: Section 2 describes the data and methods we used to perform our analysis. Our results are presented in section 3, followed by a discussion in section 4.

2. Data and Methods

2.1. GOSAT XCO_2 Retrievals

We use GOSAT short-wave infrared Fourier transform spectrometer (FTS) data from June 2009 to December 2013 (see http://www.esa-ghg-cci.org), using the v161 version of the L1B calibrated spectral radiance. To retrieve the CO_2 total column mixing ratios for these observations, we use the RemoTeC retrieval code v2.3.5 (see http://www.esa-ghg-cci.org) [*Butz et al.*, 2011]. First, a nonscattering retrieval is performed after which a first initial filtering for clouds is performed based on the retrieved ratios of the CO_2, H_2O, and O_2 columns in different retrieval windows. With these filtered data, Full Physics (FP) retrievals are performed to obtain the retrieved XCO_2 total columns. These retrievals are then more strictly filtered, and a bias correction is applied based on a comparison with ground-based FTS data from the Total Carbon Column Observing Network (TCCON) [*Guerlet et al.*, 2013]. In short this bias correction contains a constant, global offset, and a correction based on the retrieved aerosol parameters. More detailed information regarding the filters used and the comparison with respect to TCCON can be found in the Product User Guide and System Verification Report on the European Space Agency Greenhouse Gases Climate Change Initiative (ESA GHG CCI) website (http://www.esa-ghg-cci.org). We then detrend the GOSAT XCO_2 data by correcting for the year-to-year

average global XCO_2 increase. The XCO_2 interannual variability (IAV) per month is then calculated by comparing the XCO_2 in each month with the corresponding monthly average during the full period (2009–2013).

2.2. Supporting Data

To investigate possible correlations of the XCO_2 IAV with the effects of droughts and floods, we use equivalent water level derived from Gravity Recovery and Climate Experiment (GRACE) observations as a proxy for drought or flooding conditions in the region. These data are based on the Global Land Data Assimilation System to derive equivalent water level from GRACE observations [*Rodell et al.*, 2004]. Equivalent water level has been averaged to a 1 by 1° spatial resolution and 3 h temporal resolution for each month and region of interest. The time-averaged grid for January 2003 to December 2007 has been subtracted from the individual grids to derive interannually varying water levels for the period under study (2009–2013).

In addition to the GRACE equivalent water level data, we also use the ESA soil moisture CCI product version 2 [*Liu et al.*, 2011, 2012; *Wagner et al.*, 2012]. This product is a combination of both active and passive sensors (i.e., scatterometers and radiometers). These data span the period from November 1978 to December 2013, but we only use data from the beginning of 2009 to December 2013.

In recent years, satellite remote sensing of solar-induced chlorophyll fluorescence (SIF) has become feasible [*Krause and Weis*, 1991; *Joiner et al.*, 2011]. As a positive correlation between SIF and CO_2 assimilation exists [*Flexas and Medrano*, 2002; *Damm et al.*, 2010; *van der Tol et al.*, 2009], remote sensing of SIF allows for a more direct measurement of GPP globally. Here we use the SIF product derived from Global Ozone Monitoring Experiment (GOME-2) measurements for June 2009 to January 2012 [*Köhler et al.*, 2014].

Biomass burning is another important component in the carbon cycle of Australia, since relatively large areas of grasslands in the remote interior burn every year. We use the Global Fire Emissions Database (GFED) v3.1 data [*van der Werf et al.*, 2010] to estimate CO_2 emissions from biomass burning. GFED combines satellite observations of burned area and vegetation productivity from the Carnegie-Ames-Stanford approach (CASA) biogeochemical model to calculate fire emissions. Fire emission data have been used for January 2009 to December 2011.

In addition, we also use LPJ model data from the *Poulter et al.* [2014] study. These data consist of monthly global net biome production fluxes on a 0.5 by 0.5° grid. We use the data for January 2009 to December 2012.

2.3. Regions of Interest

We divide Australia in two regions in order to probe the effects of the enhanced soil moisture. The first one covers the whole continent of Australia in order to better compare our results to *Poulter et al.* [2014], while the second one encompasses Central Australia (30°S–20°S,130°E–140°E), which is covered primarily with shrubs and grasslands. Figure 1 shows a vegetation map of Australia with the central region of Australia marked in blue. As can be seen, multiple types of vegetation exist in the central semiarid part of Australia.

3. Results

The XCO_2 interannual timescale is useful for studying the origin of observed anomalies in XCO_2 that are related to El Niño. Figure 2 a shows the observed XCO_2 IAV for Central Australia. As mentioned before, midway 2010 a transition from El Niño to strong La Niña conditions occurred. This transition caused exceptionally high rainfall in most of Australia from the end of 2010 to early 2012 and is expected to have a significant effect on the biospheric carbon uptake.

3.1. Central Australia

This region comprises the most arid region of Australia, where the vegetation mostly consists of grasses and shrubs. During most of 2009, the XCO_2 IAV is around $+0.50 \pm 0.12$ ppm. Figure 2 shows that in 2010 the CO_2 emission shifted from a positive IAV to a negative IAV with a minimum XCO_2 IAV of -1 ± 0.13 ppm in October 2010 and an average negative XCO_2 IAV of -0.50 ± 0.11 ppm in the period of September 2010 to July 2012. This variation in XCO_2 shows a consistent anticorrelation with soil moisture. In 2009 the soil moisture content is lower than average (as expected during El Niño conditions). During 2010 the soil moisture starts increasing rapidly, which coincides with the transition from an El Niño to a strong La Niña phase. Late 2010 and early 2011 we see two large peaks in the soil moisture, coinciding with the strong La Niña conditions at that time. The soil moisture shows the opposite pattern to the XCO_2 IAV.

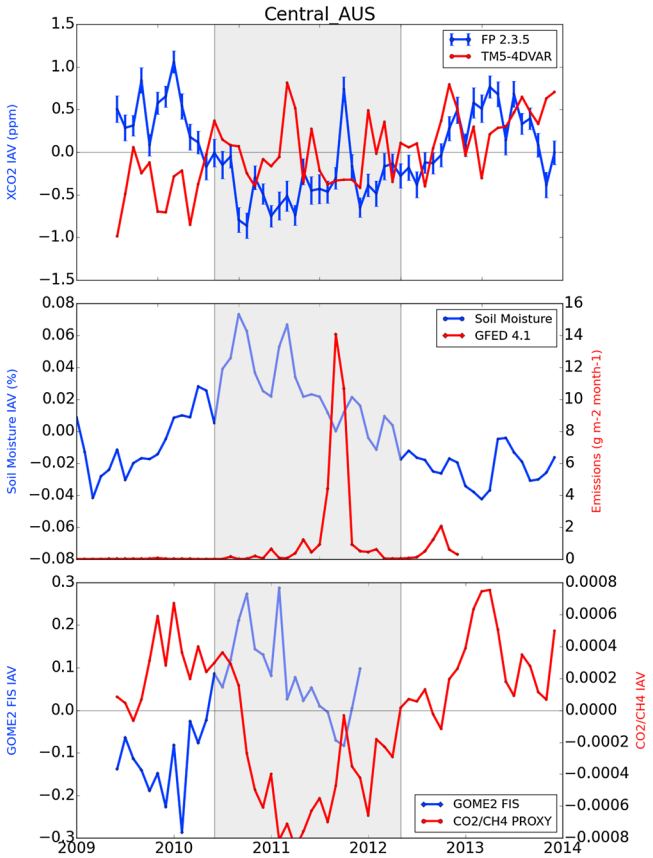

Figure 2. Interannual variability of XCO_2 (both GOSAT FP 2.3.5 and prior, TM5 4DVAR), soil moisture, biomass burning emissions (GFED 4.1), SIF (GOME-2), and retrieved XCO_2/XCH_4 ratio for Central Australia. The gray area indicates the period during which La Niña conditions were prevalent.

Figure 2 also shows SIF as retrieved from GOME-2, which correlates with vegetation greenness and was recently shown to be a good tracer of gross primary production (GPP) [*Parazoo et al.*, 2014]. The SIF data show a similar pattern as the soil moisture data. In 2009 and early 2010 the SIF IAV signal is negative, rises in the second half of 2010, and peaks at the end of 2010, coinciding with the minimum of the XCO_2 IAV. To rule out the possibility that the observed XCO_2 IAV signal is caused by aerosol-induced retrieval errors, we also plot in Figure 2 (bottom) the XCO_2/XCH_4 ratio from the nonscattering (proxy) retrieval, because this quantity is virtually insensitive to aerosol scattering. The XCO_2/XCH_4 ratio shows the same trend as the retrieved XCO_2 column, which confirms the observed trend of decreasing XCO_2 during the strong La Niña phase in the FP data. In Figure 2 (top), red shows a TM5-4DVAR forward model run using CASA-GFED fluxes. This forward run does not show the strong XCO_2 sink in 2010–2012 as seen in the GOSAT data.

Apart from the XCO_2 variation discussed above, a sharp peak is visible in October 2011 of the GOSAT data showing a large increase to almost $+1 \pm 0.13$ ppm. As can be seen from Figure 2 (middle), this peak coincides with a maximum in GFED biomass burning CO_2 emissions. As shown in *Giglio et al.* [2013], the year of 2011 was a record year for Australian bush fires (see Figure 9 of that paper). This can be explained by a period with a strong buildup of vegetation in the region before the start of the fire season. The strong peak in biomass burning emissions is therefore additional proof for the strong carbon uptake by the biosphere that took place from the second half of 2010 onward.

3.2. Biosphere Model Comparison

The results of the previous subsection raise the question whether the GOSAT-derived carbon flux IAV can be reproduced by biochemical models, such as CASA-GFED. If so, the GOSAT measurements, while still interesting, would add little to our knowledge of the interannual variability of the biosphere in Australia. In order to translate the observed XCO_2 variations to actual fluxes, we use the TM5-4DVAR inversion system. We perform two runs with this system: a forward TM5 simulation with CASA-GFED fluxes and a TM5-4DVAR

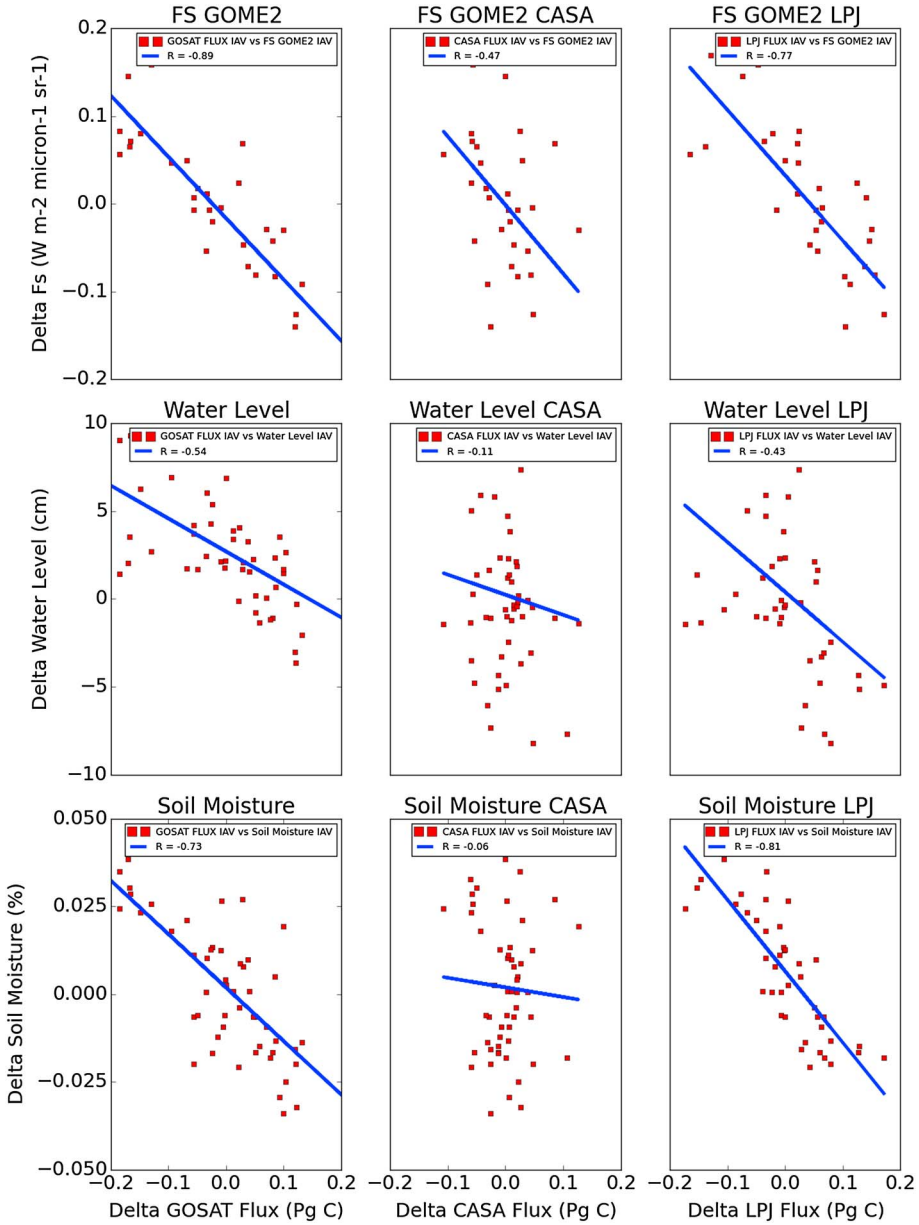

Figure 3. Correlation between land surface parameters and carbon flux IAV derived from inverse modeling of (left column) GOSAT XCO_2 data, (middle column) biosphere fluxes from CASA-GFED, and (right column) LPJ-derived NBP IAV for Central Australia.

inversion using the GOSAT XCO_2 observations to constrain the biosphere fluxes. We also quantified the correlations of each of the land surface variables with the GOSAT-derived carbon fluxes IAV and the LPJ-derived NBP, using Pearson's squared correlation coefficient. The resulting correlation coefficients can be seen in Figure 3. In the middle column the correlations with CASA-GFED carbon fluxes are shown as well. These correlations were calculated by taking monthly averages of the carbon flux IAV and the corresponding variable of interest. As can be seen the GRACE water level, ESA soil moisture, and SIF all show strong anticorrelations with the GOSAT flux IAV (−0.89, −0.54, and −0.73, respectively), as well as the LPJ flux IAV (−0.77, −0.43, and −0.81, respectively). For the CASA-GFED fluxes and SIF the anticorrelation is also significant, but for the soil moisture and GRACE water level the correlations are not significant.

Figure 4 shows the biosphere fluxes of both runs. The IAV fluxes have been smoothed using a 12 month running mean and then binned to a 3 month resolution for clarity. As can be seen the IAV of these biosphere fluxes shows significant differences between the two. The run based on the CASA-GFED model only shows

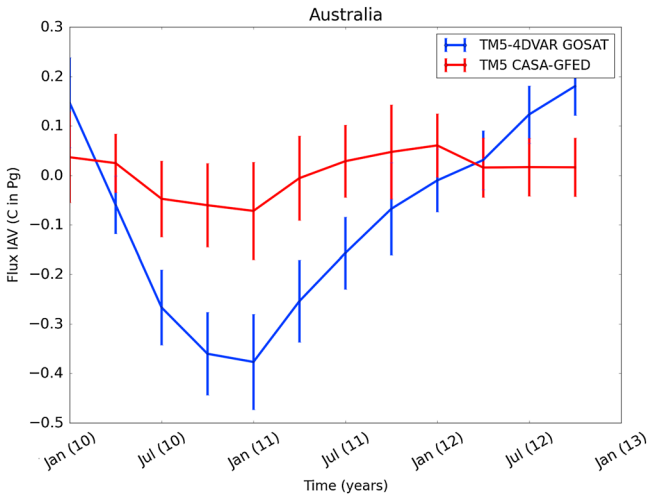

Figure 4. Carbon flux IAV for a TM5-4DVAR GOSAT-based inversion and a CASA-GFED TM5 forward model run.

very limited variability in the 3 monthly biosphere fluxes, while the GOSAT-based one shows a strong drop starting in 2010 and lasting until early 2012. Based on the calculated 3 monthly fluxes in Figure 4, we estimate the strength of the enhancement of the carbon sink to be roughly 0.77 ± 0.10 Pg C yr^{-1} or 1.5 ± 0.2 Pg C for the whole period of April 2010 to December 2011, which corresponds to 25% of the total multiyear (1990–2011) average GPP of the Australian biosphere and 1000% of the average annual net ecosystem production [*Haverd et al.*, 2013]. Compared to the enhanced LPJ sink reported in *Poulter et al.* [2014], we derived a 2011 enhancement in the sink of 0.86 ± 0.15 Pg C, which is very similar to the 0.79 Pg C quoted in that publication.

4. Discussion

Our results show a strong carbon uptake in Australia from the end of 2010 to mid-2012. This uptake coincided with record-breaking rainfall and consequent soil moisture increase that lead to increased growth of vegetation as shown by the increased SIF and the observed peak in biomass burning emissions, as well as the large increased flux uptake shown in the inversion results. Here we discuss these results in more detail.

Atmospheric CO_2 variability is driven by a wide range of processes, such as temperature, drought/flooding, and fire emissions. Recent studies [*Keeling et al.*, 1995; *Rafelski et al.*, 2009; *Keppel-Aleks et al.*, 2014] have shown a positive correlation between land temperature anomalies and the atmospheric CO_2 growth rate (in regions where vegetation growth is not limited by temperature). The latter study also showed that temperature anomalies are not the only driver and that drought/flooding events and fire emissions all contribute to net ecosystem exchange anomalies. In the case of Central Australia the main driver of vegetation growth is soil moisture content. This was already shown in *Chen et al.* [2014], who compared a long time series of soil moisture and satellite-derived NDVI and found that in arid, moisture-limited regions with low vegetation cover, NDVI strongly correlates with soil moisture, with a typical lag time of 1 month. This is also what is shown in the SIF signal, which lags behind soil moisture. This enhanced growth of the vegetation is also what led to the significant increase in biomass burning emissions in the dry season of 2011. Although these emissions are very large compared to earlier years, they do not fully offset the carbon uptake due to the enhanced vegetation growth during the analyzed years (see Figure 4).

What is clear from the inversion results is that the observed sink by GOSAT is much stronger than that from CASA-GFED, even though the CASA-GFED model also incorporates actual MODIS observations. The enhancement in the sink is comparable to that of the LPJ model in *Poulter et al.* [2014]. The difference between CASA-GFED and LPJ might be due to the higher sensitivity of the LPJ model to precipitation. This result demonstrates the added value that satellites such as GOSAT can make to the quantification of carbon flux estimates in semiarid regions. Despite the nonideal coverage of the GOSAT satellite (gaps in between sampling points), the number of high-quality, clear-sky data in this region is sufficient to detect changes in the carbon land sink. Combining these GOSAT data with a TM5-4DVAR-like inversion system and supplementary important

biospheric data, such as soil moisture, water level, SIF, and biomass burning emissions, allows us then to link and to quantify the observed changes in the XCO_2 total column, with actual changes in the biosphere.

5. Conclusions

Our results show a significant change in the carbon uptake in Australia during the La Niña phase from the end of 2010 to early 2012. Due to the record-breaking rainfall, large-scale vegetation growth occurred in the arid central region, leading to a strong carbon uptake by the land biosphere of roughly 0.77 ± 0.10 Pg C yr^{-1} or 1.5 ± 0.2 Pg C for the whole period of April 2010 to December 2011, corresponding to 1000% of the total annual net ecosystem production. The vegetation provided ample fuel for the biomass burning in the dry season of 2011, leading to a large increase in biomass burning emissions in Central Australia, also detected in the GOSAT XCO_2 IAV. After this 2 year period of increased carbon uptake, drought conditions once again returned at the end of 2012 (see Figure 2), leading to a loss of carbon uptake by the land. Semiarid regions such as the inland of Australia are very sensitive to the effects of drought/flooding conditions, usually driven by El Niño/La Niña cycles. As shown in recent work [*Poulter et al.*, 2014], the effects of climate extremes are the most severe in semiarid regions. Our results show that XCO_2 satellite observations such as by GOSAT have the ability to detect these changes in XCO_2. Combining these changes with other key variables such as soil moisture and SIF. Using inverse modeling systems allows us to link the XCO_2 changes with changes in net ecosystem exchange of carbon. Monitoring these ecosystems in the coming years provides promising opportunities for investigating how they will adapt to climate extremes in the future.

Acknowledgments

Rob Detmers acknowledges funding from the ESA Climate Change Initiative Greenhouse Gases project. Andre Butz is supported by Deutsche Forschungsgemeinschaft (DFG) through the Emmy-Noether Programme, grant BU2599/1 (RemoTeC). Luis Guanter and Philipp Köhler are supported by Deutsche Forschungsgemeinschaft (DFG) through the Emmy-Noether Programme (GlobFluo project). Access to GOSAT data was granted through the second GOSAT research announcement jointly issued by JAXA, NIES, and MOE. GFED 3.1 data were obtained through the Global Fire Emissions Database. Soil moisture data were obtained through the ESA CCI soil moisture website. GRACE data were received from http://grace.jpl.nasa.gov which used the Goddard Earth Sciences Data and Information Services Center.

The Editor thanks Peter Rayner and an anonymous reviewer for their assistance in evaluating this paper.

References

Bastos, A., S. W. Running, C. Gouveia, and R. M. Trigo (2013), The global NPP dependence on ENSO: La Niña and the extraordinary year of 2011, *J. Geophys. Res. Biogeosci.*, *118*, 1247–1255, doi:10.1002/jgrg.20100.

Basu, S., et al. (2011), The seasonal cycle amplitude of total column CO_2: Factors behind the model-observation mismatch, *J. Geophys. Res.*, *116*, D23306, doi:10.1029/2011JD016124.

Butz, A., et al. (2011), Toward accurate CO_2 and CH_4 observations from GOSAT, *Geophys. Res. Lett.*, *38*, L14812, doi:10.1029/2011GL047888.

Chen, T., R. de Jeu, Y. Liu, G. van der Werf, and A. Dolman (2014), Using satellite based soil moisture to quantify the water driven variability in NDVI: A case study over Mainland Australia, *Remote Sens. Environ.*, *140*, 330–338, doi:10.1016/j.rse.2013.08.022.

Cox, P., D. Pearson, B. Booth, P. Friedlingstein, C. Huntingford, C. D. Jones, and C. Luke (2013), Sensitivity of tropical carbon to climate change constrained by carbon dioxide variability, *Nature*, *494*(7437), 341–344, doi:10.1038/nature11882.

Crisp, D., et al. (2012), The ACOS CO_2 retrieval algorithm. Part II: Global x_{CO_2} data characterization, *Atmos. Meas. Tech.*, *5*(4), 687–707, doi:10.5194/amt-5-687-2012.

Damm, A., et al. (2010), Remote sensing of Sun-induced fluorescence to improve modeling of diurnal courses of gross primary production (GPP), *Global Change Biol.*, *16*(1), 171–186, doi:10.1111/j.1365-2486.2009.01908.x.

Delworth, T. L., and F. Zeng (2014), Regional rainfall decline in Australia attributed to anthropogenic greenhouse gases and ozone levels, *Nat. Geosci.*, *7*, 583–587, doi:10.1038/ngeo2201.

Fasullo, J. T., C. Boening, F. W. Landerer, and R. S. Nerem (2013), Australia's unique influence on global sea level in 2010–2011, *Geophys. Res. Lett.*, *40*, 4368–4373, doi:10.1002/grl.50834.

Flexas, J., and H. Medrano (2002), Drought-inhibition of photosynthesis in C_3 plants: Stomatal and non-stomatal limitations revisited, *Ann. Bot.*, *89*(2), 183–189, doi:10.1093/aob/mcf027.

Frankenberg, C., et al. (2015), The Orbiting Carbon Observatory (OCO-2): Spectrometer performance evaluation using pre-launch direct Sun measurements, *Atmos. Meas. Tech.*, *8*(1), 301–313, doi:10.5194/amt-8-301-2015.

Giglio, L., J. T. Randerson, and G. R. Werf (2013), Analysis of daily, monthly, and annual burned area using the fourth-generation global fire emissions database (GFED4), *J. Geophys. Res. Biogeosci.*, *118*, 317–328, doi:10.1002/jgrg.20042.

Guerlet, S., S. Basu, A. Butz, M. Krol, P. Hahne, S. Houweling, O. P. Hasekamp, and I. Aben (2013), Reduced carbon uptake during the 2010 Northern Hemisphere summer from GOSAT, *Geophys. Res. Lett.*, *40*, 2378–2383, doi:10.1002/grl.50402.

Haverd, V., M. R. Raupach, P. R. Briggs, J. Canadell, S. J. Davis, R. M. Law, C. P. Meyer, G. P. Peters, C. Pickett-Heaps, and B. Sherman (2013), The Australian terrestrial carbon budget, *Biogeosciences*, *10*(2), 851–869, doi:10.5194/bg-10-851-2013.

Joiner, J., Y. Yoshida, A. P. Vasilkov, Y. Yoshida, L. A. Corp, and E. M. Middleton (2011), First observations of global and seasonal terrestrial chlorophyll fluorescence from space, *Biogeosciences*, *8*(3), 637–651, doi:10.5194/bg-8-637-2011.

Keeling, C. D., T. P. Whorf, M. Wahlen, and J. van der Plichtt (1995), Interannual extremes in the rate of rise of atmospheric carbon dioxide since 1980, *Nature*, *375*, 666–670, doi:10.1038/375666a0.

Keenan, T., et al. (2012), Terrestrial biosphere model performance for inter-annual variability of land-atmosphere CO_2 exchange, *Global Change Biol.*, *18*(6), 1971–1987, doi:10.1111/j.1365-2486.2012.02678.x.

Keppel-Aleks, G., A. S. Wolf, M. Mu, S. C. Doney, D. C. Morton, P. S. Kasibhatla, J. B. Miller, E. J. Dlugokencky, and J. T. Randerson (2014), Separating the influence of temperature, drought, and fire on interannual variability in atmospheric CO_2, *Global Biogeochem. Cycles*, *28*, 1295–1310, doi:10.1002/2014GB004890.

Köhler, P., L. Guanter, and J. Joiner (2014), A linear method for the retrieval of Sun-induced chlorophyll fluorescence from GOME-2 and SCIAMACHY data, *Atmos. Meas. Tech. Discuss.*, *7*(12), 12,173–12,217, doi:10.5194/amtd-7-12173-2014.

Krause, G. H., and E. Weis (1991), Chlorophyll fluorescence and photosynthesis: The basics, *Annu. Rev. Plant Physiol. Mol. Biol.*, *42*, 313–349, doi:10.1146/annurev.pp.42.060191.001525.

Liu, Y., W. Dorigo, R. Parinussa, R. de Jeu, W. Wagner, M. McCabe, J. Evans, and A. van Dijk (2012), Trend-preserving blending of passive and active microwave soil moisture retrievals, *Remote Sens. Environ.*, *123*, 280–297, doi:10.1016/j.rse.2012.03.014.

Liu, Y. Y., R. M. Parinussa, W. A. Dorigo, R. A. M. De Jeu, W. Wagner, A. I. J. M. van Dijk, M. F. McCabe, and J. P. Evans (2011), Developing an improved soil moisture dataset by blending passive and active microwave satellite-based retrievals, *Hydrol. Earth Syst. Sci.*, *15*(2), 425–436, doi:10.5194/hess-15-425-2011.

Meirink, J. F., P. Bergamaschi, and M. C. Krol (2008), Four-dimensional variational data assimilation for inverse modelling of atmospheric methane emissions: Method and comparison with synthesis inversion, *Atmos. Chem. Phys.*, *8*(21), 6341–6353, doi:10.5194/acp-8-6341-2008.

Parazoo, N. C., K. Bowman, J. B. Fisher, C. Frankenberg, D. B. A. Jones, A. Cescatti, Ó. Pérez-Priego, G. Wohlfahrt, and L. Montagnani (2014), Terrestrial gross primary production inferred from satellite fluorescence and vegetation models, *Global Change Biol.*, *20*(10), 3103–3121, doi:10.1111/gcb.12652.

Poulter, B., et al. (2014), Contribution of semi-arid ecosystems to interannual variability of the global carbon cycle, *Nature*, *509*(7502), 600–603, doi:10.1038/nature13376.

Rafelski, L. E., S. C. Piper, and R. F. Keeling (2009), Climate effects on atmospheric carbon dioxide over the last century, *Tellus, Ser. B*, *61*, 718–731, doi:10.1111/j.1600-0889.2009.00439.x.

Rodell, M., et al. (2004), The global land data assimilation system, *Bull. Am. Meteorol. Soc.*, *85*, 381–394, doi:10.1175/BAMS-85-3-381.

Rotenberg, E., and D. Yakir (2010), Contribution of semi-arid forests to the climate system, *Science*, *327*(5964), 451–454, doi:10.1126/science.1179998.

Sitch, S., et al. (2003), Evaluation of ecosystem dynamics, plant geography and terrestrial carbon cycling in the LPJ dynamic global vegetation model, *Global Change Biol.*, *9*(2), 161–185, doi:10.1046/j.1365-2486.2003.00569.x.

van der Tol, C., W. Verhoef, J. Timmermans, A. Verhoef, and Z. Su (2009), An integrated model of soil-canopy spectral radiances, photosynthesis, fluorescence, temperature and energy balance, *Biogeosciences*, *6*, 3109–3129.

van der Werf, G. R., J. T. Randerson, L. Giglio, G. J. Collatz, M. Mu, P. S. Kasibhatla, D. C. Morton, R. S. Defries, Y. Jin, and T. T. van Leeuwen (2010), Global fire emissions and the contribution of deforestation, savanna, forest, agricultural, and peat fires (1997–2009), *Atmos. Chem. Phys.*, *10*, 11,707–11,735, doi:10.5194/acp-10-11707-2010.

Wagner, W., W. Dorigo, R. de Jeu, D. Fernandez, J. Benveniste, E. Haas, and M. Ertl (2012), Fusion of active and passive microwave observations to create an essential climate variable data record on soil moisture, *ISPRS Ann. Photogramm. Remote Sens. Spatial Inf. Sci.*, *I–7*, 315–321, doi:10.5194/isprsannals-I-7-315-2012.

Wang, W., P. Ciais, R. R. Nemani, J. G. Canadell, S. Piao, S. Sitch, M. A. White, H. Hashimoto, C. Milesi, and R. B. Myneni (2013), Variations in atmospheric CO_2 growth rates coupled with tropical temperature, *Proc. Natl. Acad. Sci. U.S.A.*, *110*(32), 13,061–13,066, doi:10.1073/pnas.1219683110.

Yoshida, Y., Y. Ota, N. Eguchi, N. Kikuchi, K. Nobuta, H. Tran, I. Morino, and T. Yokota (2011), Retrieval algorithm for CO_2 and CH_4 column abundances from short-wavelength infrared spectral observations by the Greenhouse Gases Observing Satellite, *Atmos. Meas. Tech.*, *4*(4), 717–734, doi:10.5194/amt-4-717-2011.